Indian Journal of Pure & Applied Physics
Vol. 53, February 2015, pp. 102-109

Electronic structure and elastic properties of $ATiO_3$ (A = Ba, Sr, Ca) perovskites: A first principles study

Anup Pradhan Sakhya[1]*, Jameson Maibam[2], Sujoy Saha[1], Sadhan Chanda[1], Alo Dutta[1], B Indrajit Sharma[2], R K Thapa[3] & T P Sinha[1]

[1]Department of Physics, Bose Institute, 93/1, Acharaya Prafullachandra Road, Kolkata 700 009, India

[2]Department of Physics, Assam University, Silchar, Assam 788 011, India

[3]Department of Physics, Mizoram University, Tanhril, Aizawl 796 009, Mizoram, India

*E-mail: npshakya31@gmail.com

Received 4 September 2013; revised 2 April 2014; accepted 25 September 2014

The elastic constants of perovskite oxides $ATiO_3$ (A = Ba, Sr, Ca) in the cubic phase are calculated using the full-potential linearized augmented plane wave method within the density functional theory in its generalized gradient approximation. The modified Becke-Johnson potential (TB-mBJ) is applied for the electronic structure calculation. The calculated results are used to obtain the Young's modulus, shear modulus, Poisson's ratio, isotropic shear modulus, longitudinal, transverse and average sound velocities, Zener anisotropy factor, Kleinman parameter and Debye temperature of the systems. The calculated results are compared with the available experimental data.

Keywords: Density functional theory, Becke-Johnson potential, Perovskite oxides, Elastic constant

1 Introduction

ABO_3 type perovskite oxides are very important materials for their numerous technological applications in electro-optics, waveguides, laser frequency doubling, high capacity computer memory cells etc[1,2]. The response of these oxides to an applied stress is determined by the elastic constants (C_{ij}) which give the information about the binding characters between the adjacent atomic planes, the anisotropic character of the bonding and structural stability of the systems. C_{ij} can easily be determined from first principles calculations using density functional theory (DFT). Using the values of C_{ij}, the isotropic bulk modulus, shear modulus, Young's modulus and the Poisson's ratio of the materials can be obtained.

A well known example of perovskite oxides is $ATiO_3$ (A = Ba, Sr, Ca), where $BaTiO_3$ (BT) undergoes a sequence of phase transitions with increasing temperature at 183, 278 and 393 K. Its structure transforms from rhombohedral to orthorhombic, from orthorhombic to tetragonal and from tetragonal to cubic, respectively[2]. Similarly, $CaTiO_3$ (CT) is orthorhombic with space group Pbnm below 1380 K and belongs to another orthorhombic space group Cmcm between 1380 and 1500 K. At 1500 K, it transforms into tetragonal phase and finally above 1580 K, it becomes cubic[3]. $SrTiO_3$ (ST) deviates from that of BT and CT as it has simple cubic perovskite structure at high temperature and goes through an anti-ferrodistortive AFD transition at 105 K to a tetragonal phase in which the oxygen octahedra have rotated by a small angle along the *c*-axis in opposite sense in neighbouring unit cells[2]. BT has a wide range of applications from dielectric capacitors to nonlinear optic devices[2]. ST has been attracted for fundamental research and perspective application in the field of ferroelectricity, optoelectronics and microelectronics as micro-capacitors, ultrathin gate chips, optical switches and so on[4-8]. CT is widely used in electronic ceramic materials and in immobilizing high-level radioactive waste[9]. It has also been widely used as an additive to modify the compositions of ferroelectric perovskite BTwith the aim of tailoring their properties for various applications[10].

Recently, the relative enthalpy among different structures of CT has been studied by Moriwake *et al*[11]. using DFT within the local density approximation (LDA). The comparative phonon symmetry analysis of BT in four phases has been performed by Evarestov and Bandura using DFT in its LDA, generalized gradient approximation (GGA) and hybrid exchange correlation approximation[12]. The

optimization of the sintering temperature of BT has been studied by Sreenivasulu *et al*[13]. A theoretical study of magnetization in non-magnetic cubic perovskite ST induced by vacancies in Sr, Ti and oxygen sublattices has been studied by Shein *et al*[14]. within the GGA. Bousquet *et al*[15]. have reported a first-principles study of $BaTiO_3$/BaO superlattices for a wide range of periodicities using LDA.

The mechanical properties of these oxides are important in the overall evaluation of the quality and suitability of the material to a particular application. Hence, the structural, elastic and electronic properties of these titanates have been studied. In the present paper, a detailed study of structural, elastic, and mechanical properties of $ATiO_3$ in the cubic phase has been performed. The TB-mBJ potential is applied to obtain their band structures. The obtained results are compared with the observed experimental data.

2 Computational Methods

The full-potential linearized augmented plane wave (FP-LAPW) method[16] as implemented in WIEN2K was applied for electronic structure calculations of $ATiO_3$. We have used the Tran and Blaha modified Becke-Johnson potential[17-19] (TB-mBJ) for calculating the electronic properties of the materials whereas the elastic properties are calculated using the generalized gradient approximation (GGA) of Perdew, Burke and Ernzerhof[20] (PBE). TB-mBJ is a newly developed semi-local exchange-correlation functional which uses information from kinetic energy density in addition to the charge density as employed in standard GGA. These TB-mBJ functionals come in the framework of Kohn Sham formalism and they are computationally less expensive as compared to hybrid functionals. The TB-mBJ functionals cannot be used for total energy calculations but yield improved band gaps in a wide variety of materials[17-19,21]. For every case, the wave functions inside the muffin-tin spheres (which are expanded into spherical harmonics) are taken up to l =10 and the value of the parameter $R_{mt}K_{max}$ was chosen to be 8 which controls the size of the basis sets in these calculations. Here, K_{max} is the maximum value of the reciprocal lattice vector used in the plane wave expansion and R_{mt} is the smallest atomic sphere. The calculations were performed at the equilibrium lattice constants that are determined from the plot of total energy against the unit cell volume by fitting to the Birch-Murnaghan equation of state[22]. For the calculation of elastic constants, we have used the procedure of Birch[23]. Muffin-tin sphere radii (RMT) for Ba, Sr, Ca, Ti and O are listed in Table 1.

3 Results and Discussion

3.1 Structural properties

Figure 1 shows the total energy curve as a function of unit cell volume for BT, ST and CT, respectively. The optimized lattice constants, isothermal bulk modulii, its pressure derivative were calculated by fitting the total energy to Birch Murnaghan equation of state[22] defined as:

$$E(V) = E_0 + \frac{9V_0B_0}{16}\left\{\left[\left(V_0/V\right)^{2/3}-1\right]^3 B_0' + \left[\left(V_0/V\right)^{2/3}-1\right]^2\left[6-4\left(V_0/V\right)^{2/3}\right]\right\} \quad \ldots(1)$$

where V_0 is the equilibrium volume and B_0 is the bulk modulus and is given by $B_0 = -V(\delta P/\delta V)_T$ evaluated at volume V_0. B_0' is the pressure derivative of B_0 also evaluated at volume V_0.

The structural parameters obtained from volume optimization are given in Table 1. It is found that the equilibrium lattice constants of BT, ST and CT are almost the same as the experimental value. The bulk modulus is a fundamental physical property of the solids and it can be used as a measure of the average bond strengths of atoms of crystals.

3.2 Elastic properties

It is well known that the total energy of a crystal in the strained state is given by[25]:

Table 1 — Muffin tin radius (RMT) and bulk modulus of $BaTiO_3$, $SrTiO_3$ and $CaTiO_3$

Compounds	Lattice constants (Å)	RMT (a.u.)	Bulk modulus B (GPa)	References
$BaTiO_3$	4.024	Ba = 2.5, Ti = 1.94, O = 1.72	166	Present work
	4.0		162	Expt. [24]
$SrTiO_3$	3.94	Sr = 2.5, Ti = 1.9, O = 1.69	175	Present work
	3.89		179	Expt. [24]
$CaTiO_3$	3.88	Ca = 2.5, Ti = 1.88, O = 1.67	179	Present work
	3.91			Expt. [3]

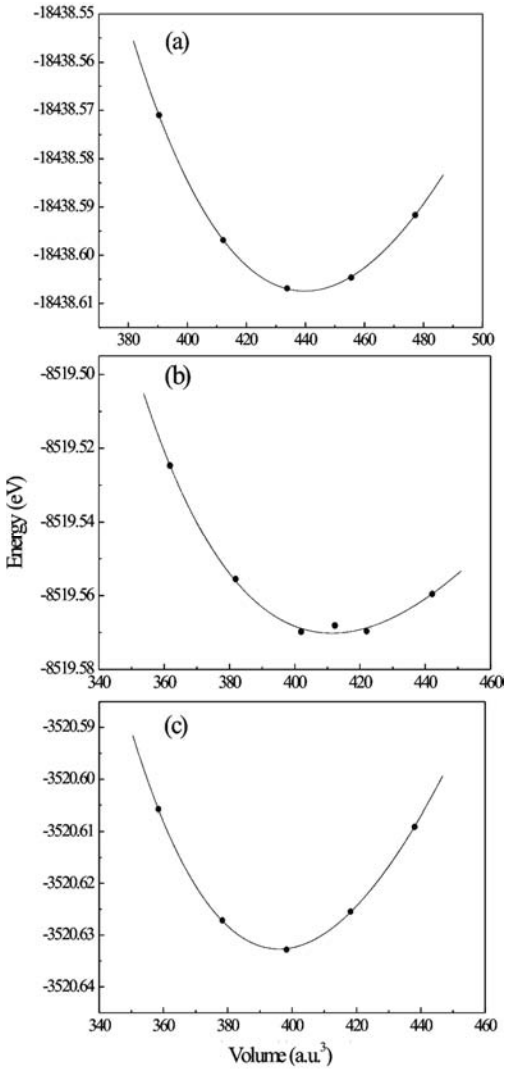

Fig. 1 — Total energy as a function of lattice constant of (a) $BaTiO_3$, (b) $SrTiO_3$ and (c) $CaTiO_3$

$$E_{tot} = E_{tot}^0 + P(V - V_0) + \phi_e \quad \ldots(2)$$

where E_{tot}^0 and V_0 are the total energy and volume of unstrained crystal, V is volume of the strained lattice and P and ϕ_e are the pressure and elastic energy, respectively defined as:

$$P = -(\partial E_{tot}^0 / \partial V)_{V_0} \quad \ldots(3)$$

and

$$\phi_e = \frac{V}{2} C_{ijkl} \varepsilon_{ij} \varepsilon_{kl} \quad \ldots(4)$$

(where $i, j, k, l = 1,2,3$)

Further, ϕ_e is modified in Voigt's two suffix notations as:

$$\phi_e = \frac{V}{2} C_{ij} \varepsilon_i \varepsilon_j \quad \ldots(5)$$

where C_{ij} are elastic moduli and can be obtained as:

$$C_{ij} = \frac{1}{V_0} \frac{\partial^2 E_{tot}}{\partial_{\varepsilon_i} \partial_{\varepsilon_j}} \quad \ldots(6)$$

A cubic crystal has only three independent elastic constants, namely, C_{11}, C_{12} and C_{44}. Once we have calculated the three elastic constants namely C_{11}, C_{12} and C_{44}, the bulk modulus B can be obtained by the formula:

$$B = \frac{1}{3}(C_{11} + 2C_{12}) \quad \ldots(7)$$

The Zener anisotropy factor A, Poisson's ratio υ, Young's modulus Y, isotropic shear modulus G, Kleinman parameter ζ and shear modulus C' can be calculated using the following relations[26]:

$$A = \frac{2C_{44}}{C_{11} - C_{12}} \quad \ldots(8)$$

$$\upsilon = \frac{1}{2}\left(\frac{B - \frac{2}{3}G}{B + \frac{1}{3}G} \right) \quad \ldots(9)$$

$$Y = \frac{9GB}{G + 3B} \quad \ldots(10)$$

and

$$G = \frac{G_V + G_R}{2} \quad \ldots(11)$$

where G_V is Voigt's shear modulus corresponding to the upper bound of G values and G_R is Reuss's shear modulus corresponding to the lower bound of G values. They can be expressed as:

$$G_V = \frac{C_{11} - C_{12} + 3C_{44}}{5} \quad \ldots(12)$$

$$\frac{5}{G_R} = \frac{4}{(C_{11} - C_{12})} + \frac{3}{C_{44}} \quad \ldots(13)$$

The Kleinman parameter ζ describes the relative positions of cation and anion sub lattices under volume conserving strain distortions for which positions are not fixed by symmetry and can be expressed as:

$$\zeta = \frac{C_{11} + 8C_{12}}{7C_{11} + 2C_{12}} \quad \ldots(14)$$

and shear modulus[27] is given by:

$$C' = \frac{C_{11} - C_{12}}{2} \quad \ldots(15)$$

The values of C_{ij} are listed in Table 2. It is well known that for cubic crystal structure, the necessary conditions for mechanical stability[30,31] are: $(C_{11}-C_{12})>0$, $(C_{11}+2C_{12})>0$, $C_{11}>0$ and $C_{44}>0$. These conditions are well satisfied for the observed values of C_{11}, C_{12} and C_{44} of the materials. Thus, these materials have mechanically stable perovskite structure. The calculated values of density, Zener anisotropy factor A, Poisson's ratio υ, Kleinman parameter ζ, Young's modulus Y and shear modulus C' of the materials are listed in Table 3.

Higher values of Young's modulus in comparison to the bulk modulus for BT, ST and CT indicate that these materials are hard to be broken[33]. The hardness of a material can also be predicted in terms of isotropic shear modulus. Since the isotropic shear modulus G represents the resistance to plastic deformation while the bulk modulus B represents the resistance to fracture, the value B/G was proposed[34] as an empirical malleability measure of polycrystalline materials. Accordingly, a material is brittle (ductile) if the B/G ratio is less (more) than 1.75. The values of the B/G for BT, ST and CT in cubic structures are found to be 1.53, 1.56 and 1.75, respectively. This indicates that BT and ST are brittle while CT is ductile.

The Zener anisotropy factor which is a measure of the degree of anisotropy in the solid structure is maximum for BT among these materials and indicates that BT has the highest anisotropic character followed by ST and CT. The values of the Poisson's ratio are indicative of the degree of directionality of the covalent bonds. The value of the Poisson's ratio is small (υ= 0.1) for covalent materials, whereas for ionic materials[35] a typical value of υ is 0.25. The calculated Poisson's ratios for BT, ST and CT are 0.23, 0.24 and 0.26, respectively. Therefore, the ionic contribution to inter atomic bonding for these compounds is dominant. It has been reported by Fu *et al*[36]. that for central force solids the lower and upper limits for υ are 0.25 and 0.5, respectively. The value of υ for CT indicates that inter atomic forces are central forces in this compound. The Kleinman parameter[37] ζ quantifies internal strain and thus indicates the relative ease of bond bending against bond stretching. It also implies resistance against bond bending or bond angle distortion. In a system, minimizing bond bending leads to $\zeta = 0$ and minimizing bond stretching leads to $\zeta = 1$. In the present study, the parameter ζ is found to be 0.49 for BT, 0.44 for ST and 0.43 for CT. It is clear that CT shows slightly more resistance to bond bending or bond angle distortion as compared to ST, whereas BT shows the lowest resistance against

Table 2 — Calculated elastic constants of $BaTiO_3$, $SrTiO_3$ and $CaTiO_3$

Compounds	Elastic constants (GPa)			References
	C_{11}	C_{12}	C_{44}	
$BaTiO_3$	295	100	116	Present work
	255	82	108	Expt. [28]
$SrTiO_3$	334	96	108	Present work
	317	102.5	123.5	Expt. [29]
$CaTiO_3$	342	97	91	Present work

Table 3 — Calculated values of density ρ, Zener anisotropy factor A, Poisson's ratio υ, Kleinman parameter ζ, Young's modulus Y, and shear modulus C' of $BaTiO_3$, $SrTiO_3$ and $CaTiO_3$

Compounds	ρ (kg/m^3)	A	υ	ζ (kg/m^3)	Y (GPa)	C' (GPa)	References
$BaTiO_3$	5948	1.197	0.23	0.49	266.81	97.25	Present work
Expt.							
$SrTiO_3$	5003	0.91	0.24	0.44	277.44	118.79	Present work
	5120	Expt.(Ref.29)					
$CaTiO_3$	3851	0.74	0.26	0.43	257.52	122.40	Present work
	3940				280	Expt. (Ref.32)	

bond bending or bond angle distortion among all the materials.

The Debye temperature is known to be an important fundamental parameter closely related to many physical properties, such as specific heat and melting temperature. At low temperatures, the vibrational excitations arise solely from acoustic vibrations. Hence, at low temperatures the Debye temperature calculated from elastic constants is the same as that determined from specific heat measurements. The Debye temperature θ_D is calculated from the elastic constants data using the average sound velocity υ_m, by the following common relation[38]:

$$\theta_D = \frac{h}{k}\left[\frac{3n}{4\pi}\left(\frac{N_A\rho}{M}\right)\right]^{1/3}\upsilon_m \qquad \ldots(16)$$

where h is Planck's constant, k the Boltzmann's constant, N_A Avogadro's number, n the number of atoms per formula unit, M the molecular mass per formula unit, $\rho = (M/V)$ is the density, and υ_m is given[39] as:

$$\upsilon_m = \left[\frac{1}{3}\left(\frac{2}{\upsilon_t^3}+\frac{1}{\upsilon_l^3}\right)\right]^{1/3} \qquad \ldots(17)$$

where υ_l and υ_t are the longitudinal and the transverse elastic wave velocities, respectively, which are obtained from Napier's equations[40]:

$$\upsilon_l = \left(\frac{3B+4G}{3\rho}\right)^{1/2} \qquad \ldots(18)$$

$$\upsilon_t = \left(G/\rho\right)^{1/2} \qquad \ldots(19)$$

The calculated values of the Debye temperature in the present formalism are presented in Table 4 indicating that the Debye temperature of CT is the highest followed by ST and BT. The average longitudinal, transverse sound velocities have been calculated using Eqs (17-19), respectively and are listed in Table 4. Debye temperature is directly related to the average sound velocity. Thus, greater the average sound velocity, greater is the Debye temperature. Furthermore, Debye temperature decreases from CT to BT due to decrease in the average velocity υ_m, which is an effect of increase in atomic weight. The calculated values of all the above parameters are compared with the experimental data wherever available.

3.3 Band structure and density of states

The band structure and the total density of states of $ATiO_3$ compounds calculated using both PBE and TB-mBJ functionals are shown in Figs 2-5.

The energy scale is in eV and the origin of energy was arbitrarily set to be at the valence band (VB) maximum defined as Fermi level. All the compounds under study are found to be insulators with an indirect

Table 4 — Calculated values of the isotropic shear modulus G, longitudinal sound velocity υ_l, transverse sound velocity υ_t, average sound velocity υ_m and Debye temperature θ_D

Compunds	G (GPa)	υ_l (m/s)	υ_t (m/s)	υ_m (m/s)	θ_D (K)
$BaTiO_3$	108.34	7219.03	4268.04	4728.14	598.47
$SrTiO_3$	112.23	8057.1	4736.14	5249.52	679.44
$CaTiO_3$	102.19	9045.42	5151.43	5725.82	750.54

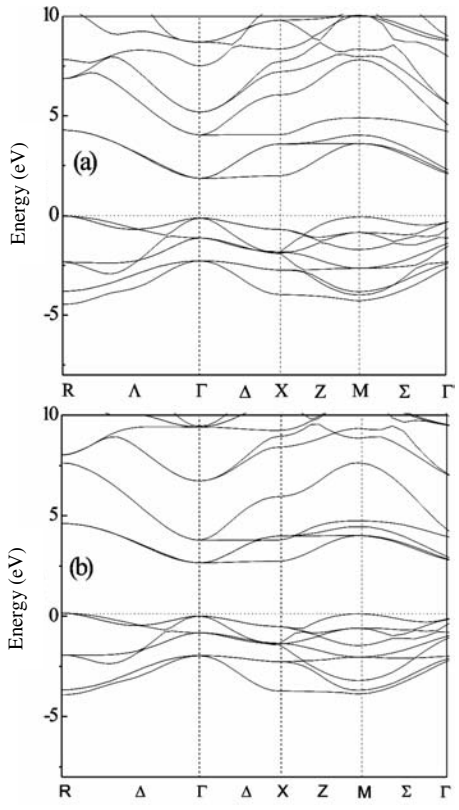

Fig. 2 — (a) PBE band structure, (b) TB-mBJ band structure for $BaTiO_3$

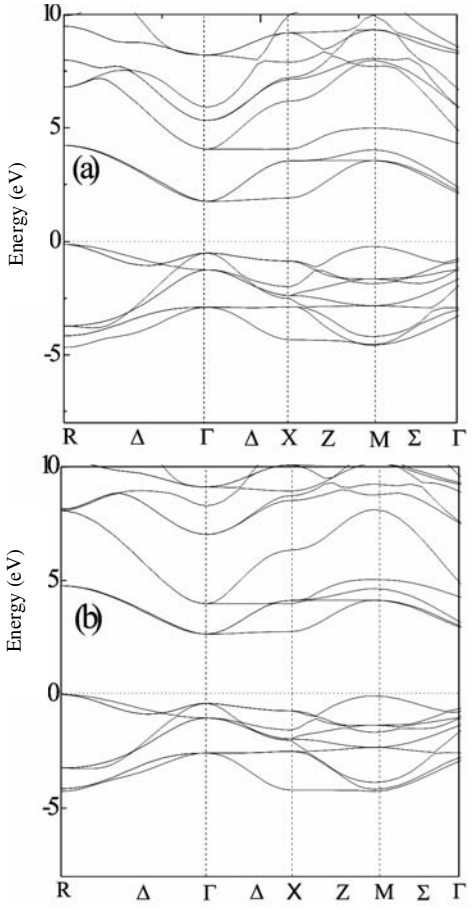

Fig. 3 — (a) PBE band structure, (b) TB-mBJ band structure for $SrTiO_3$

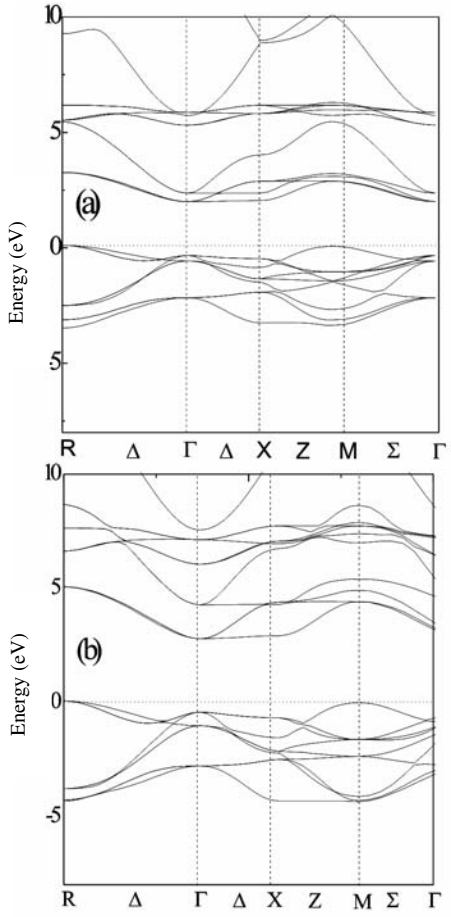

Fig. 4 — (a) PBE band structure, (b) TB-mBJ band structure for $CaTiO_3$

band gap between valence band maximum (VBM) at *R* point and the conduction band minimum (CBM) at Γ point. The band gaps obtained by using PBE functional are less than the experimental values. (The experimental band gap for BT is 2.83 eV (Ref. 41), for ST is 3.2 (Ref. 42) and for CT is 3.5 (Ref. 43). On the other hand, when the TB-mBJ functional is used the band gap increases considerably from 1.79 to 2.7 eV for BT, from 1.63 to 2.7 eV for ST and from 1.95 to 2.78 eV for CT which is very close to the experimental values. This improvement in the band gap using TB-mBJ is clearly seen from the density of states (DOS) plots. In Fig. 5, the DOS obtained using both the functionals are shown.

The partial density of states obtained using TB-mBJ is shown in Fig. 6. The energetic positions of the bands and the band gaps obtained by using TB-mBJ potential have changed considerably as compared to that obtained by using PBE. The Ti 3*d* conduction bands are shifted upwards in general leading to an increase in the band gap. In cubic BT, ST and CT nine valence bands near the Fermi level are the three triply degenerate levels derived from O-2*p* orbitals. These splittings are produced by the crystal field and the electrostatic interaction between O-2*p* orbitals.

For BT, the region near the Fermi level, i.e., top of the valence band (VB) spreads from −4.0 to 0 eV and have O-2*p* like character with very less contribution from Ti-3*d* and Ba-3*d* states. The lower part of the CB is mainly composed of Ti-3*d* orbitals with small contribution from O-2*p* states and the higher part of the conduction band is mainly derived from Ba-3d states. In the case of ST, the top of the valence bands which spreads around −4.29 to 0 eV is dominated by the O-2*p* states hybridized with the Ti-3*d* and Sr-3*d* states. The lower part of the CB is mainly composed of Ti-3*d* orbitals hybridized with O-2*p* states and the higher part of the conduction band is mainly derived from Sr 3*d* states.

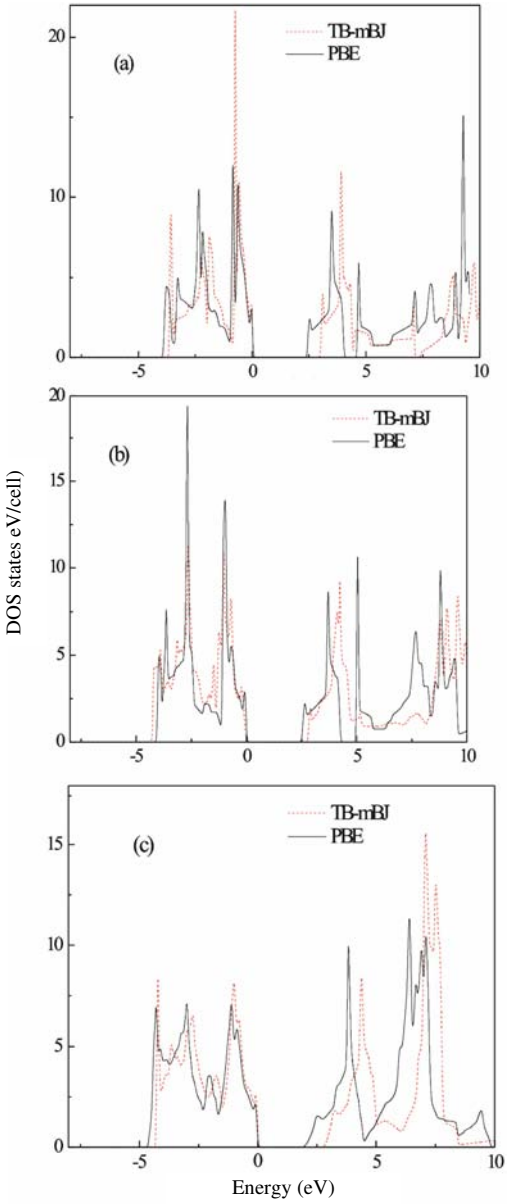

Fig. 5 — Total DOS with PBE (solid line), TB-mBJ (dotted line) for (a) $BaTiO_3$, (b) $SrTiO_3$ and (c) $CaTiO_3$

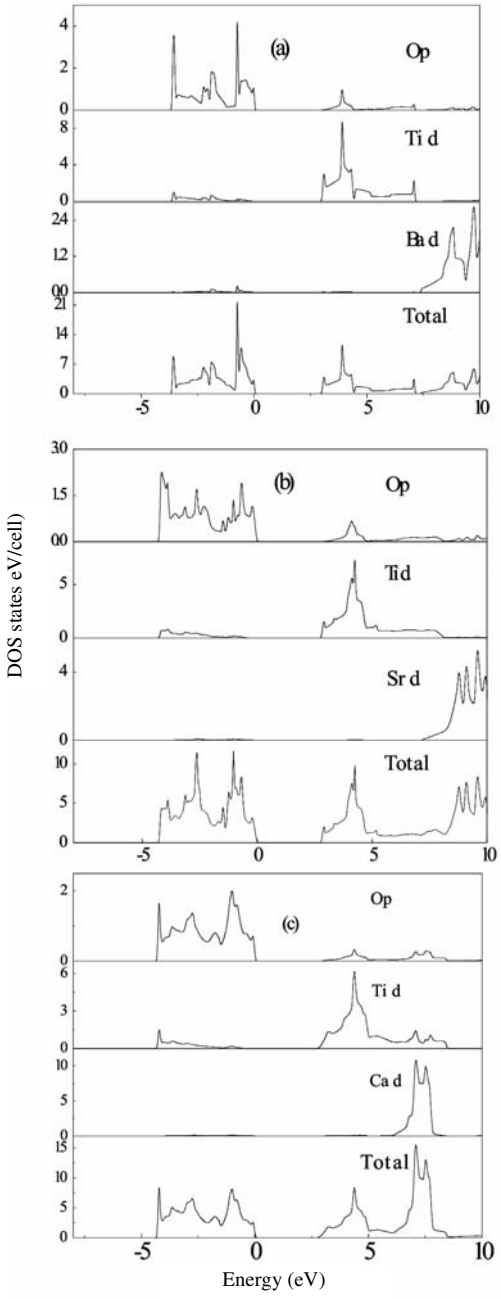

Fig. 6 — Total DOS and partial DOS with TB-mBJ for (a) $BaTiO_3$, (b) $SrTiO_3$ and (c) $CaTiO_3$

For CT, the top of the VB region extends from –4.4 to 0 eV and is dominated mostly by the O-2*p* like states hybridized with the Ti-3*d* states and Ca-3*d* states. The lower part of the CB is mainly composed of Ti-3*d* orbitals hybridized with O-2*p* states and the higher part of the CB is mainly derived from Ca-3*d* states. The general features of the energy bands and density of states of $ATiO_3$ are quite similar. In all the compounds, the orbital character of the VB is primarily derived from oxygen 2p orbitals, with metal-oxygen bonding states at the bottom of the VB and oxygen non-bonding states at the top of the VB. The CB has strong metallic d-orbital character, originating from the anti-bonding metal-oxygen interactions. CB minima of all the three compounds are dominated by Ti-3*d* states. Bandwidth of the top most VB region for the compounds under study is the largest for CT and the lowest for BT.

4 Conclusions

The elastic constants of BT, ST and CT in the cubic phase have been calculated by using full-potential linearized augmented plane wave method. The elastic constants obtained from the calculations are very close to the experimental values. Using the values of the elastic constants, the bulk modulus, Zener anisotropy, Poisson's ratio, Kleinman parameter, Young's modulus and shear modulus are obtained and found to be in good agreement with the available experimental values. The isotropic shear modulus, density, Debye temperature, longitudinal, transverse and average sound velocities have also been calculated. Since the experimental data for various parameters are not available in the literature, so a comparison of all the calculated parameters could not be done. The electronic properties of $ATiO_3$ (A = Ba, Sr, Ca) using both PBE and TB-mBJ have been investigated. These compounds have the indirect band gap with valence band maximum at *R* point and the conduction band minimum at Γ point. The top of the valence band of all the compounds are dominated by O-2*p* states and the lower part of the conduction band by Ti-3*d* states. It is observed that the TB-mBJ significantly improves the band gap which is very close to the experimental energy gaps.

Acknowledgement

Anup Pradhan Sakhya acknowledges Department of Science and Technology for Inspire Fellowship for financial support. Sujoy Saha acknowledges the financial support provided by the UGC, New Delhi in the form of SRF. Alo Dutta thanks to Department of Science & Technology, Government of India, New Delhi for providing the financial support through DST Fast Track Project under grant No. SR/FTP/PS-032/2010.

References

1 Noguera C, *Physics and Chemistry at Oxide Surfaces* (Cambridge University Press, Cambridge), 1996.
2 Lines M E & Glass A M, *Principles and Applications of Ferroelectrics and Related Materials* (Clarendon Press, Oxford), 1977.
3 Kennedy B J, Howard C J & Chakoumakos B C, *J Phys Condensed Matter*, 11 (1999) 1479.
4 Bednorz G & Muller K A, *Phys Rev Lett*, 52 (1984) 2289.
5 McKee R A, Walker F J & Chisholm M F, *Science*, 293 (2001) 486.
6 Sirenko A A, Bernhard C, Goinik A *et al*., *Nature*, 404 (2000) 373.
7 Vendik O G & Zubko S P, *Appl Phys Lett*, 82 (1997) 4475.
8 Li H C, Si W, West A D & Xi X X, *Appl Phys Lett*, 73 (1998) 464.
9 Ringwood A E, Kesson S E, Reeve K D *et al*., *Radioactive Waste Forms for the Future* (Elsevier, Amsterdam), 1988 p. 233.
10 Fu D, Itoh M & Koshihara S, *J Phys Condensed Matter*, 22 (2010) 052204.
11 Moriwake H, Fisher C A J, Kuwabara A *et al., Journal of the Korean Physical Society*, 59 (2011) 2497.
12 Evarestov R A & Bandura A V, *J Comput Chem*, 33 (2012) 1123.
13 Sreenivasulu A, Prasad T N V K V & Buddhudu S, *Indian J Pure & Appl Phys,* 45 (2007) 741.
14 Shein I R & Ivanovskii A L, *Phys Lett A*, 371 (2007) 155.
15 Bousquet E, Junquera J & Ghosez P, *Phys Rev B*, 82 (2010) 045426.
16 Blaha P, Schwarz K, Madsen G K H *et al*., *WIEN2K, An augmented plane wave plus local orbitals program for calculating crystal properties* (Schwarz K. Technical Universitat, Wien, Austria), 2001 ISBN 3-9501031-1-2.
17 Koller D, Tran F & Blaha P, *Phys Rev B*, 83 (2011) 195134.
18 Tran F & Blaha P, *Phys Rev Lett*, 102 (2009) 226401.
19 Dixit H, Saniz R, Cottenier S *et al., J Phys Condensed Matter*, 24 (2012) 205503.
20 Perdew J P, Burke K & Ernzerhof M, *Phys Rev Lett*, 77 (1996) 3865.
21 Singh D J, *Phys Rev B,* 82 (2010) 155145.
22 Birch F, *Phys Rev*, 71 (1947) 809.
23 Birch F, *J Appl Phys,* 9 (1938) 279.
24 Hellwege K H & Hellwege A M, *Landolt-Bornstein Numerical Data and Functional Relationships in Science and Technology, New Series, Group III*, (Springer-Verlag, Berlin), 1969, Vol 3.
25 Charpin T, *A package for Calculating elastic tensors of cubic phase using WIEN: Laboratory of geometrix* F-75252 (Paris, France), 2001.
26 Mayer B, Anton H, Bott E *et al*., *Intermetallics*, 11 (2003) 23.
27 Harisson W A, *Electronic Structure and the Properties of solids* (Dover Publications Inc,
28 New York), 1989.
29 Berlincourt D & Jaffe H, *Phys Rev*, 111 (1958) 143.
30 Piskunov S, Heifets E, Eglitis R I & G Borstel, *Comput Mater Sci*, 29 (2004) 165.
31 Wallace D C, *Thermodynamics of crystals* (*John Wiley & Sons Inc, New York*), 1972.
32 Bhalla V, Kumar R, Tripathy C & Singh D, *Int J Mod Phys B,* 27 (2013) 1350116.
33 Degtyareva E V, Verba L I, Gulko N V *et al*., *Inorg Mater*, 13 (1977) 853.
34 Yuan P F & Ding Z J, *Physica B*, 403 (2008) 1996.
35 Pugh S F, *Phil Mag*, 45 (1954) 833.
36 Bannikov V V, Shein I R & Ivanovskii A L, *Phys Status Solidi Rapid Res Lett*, 3 (2007) 89.
37 Fu H, Li D, Peng F *et al*., *Comput Mater Sci*, 44 (2008) 774.
38 Kleinman L, *Phys Rev B*, 12 (1962) 2614.
39 Johnston E, Keeler G, Rollins R & Spicklemeire S, *Solid State Physics Simulations*, *A Consortium for Upper Level Physics Software* (Wiley, New York), 1996.
40 Anderson O L, *J Phys Chem Solids*, 24 (1963) 909.
41 Schreiber E, Anderson O L & Soga N, *Elastic Constants and Their Measurements* (McGraw-Hill, New York), 1973.
42 Wemple S H, *Phys Rev B*, 2 (1970) 2679.
43 Lee C, Yahia J & Brebner J L, *Phys Rev B*, 3 (1971) 2525.
44 Ueda K, Yanagi H, Hosono H & Kawazoe H, *J Phys Condensed Matter*, 10 (1998) 3669.